

Behavior of fibre reinforced cementitious material-filled steel tubular columns

O.F. Kharoob* and M.H. Taman

Department of Structural Engineering, Faculty of Engineering, Tanta University, Tanta, Egypt

(Received November 09, 2016, Revised January 16, 2017, Accepted January 20, 2017)

Abstract. This paper presents an experimental study, investigating the compressive behavior of glass-fibre reinforced and unreinforced cementitious material-filled square steel tubular (GFCMFST and CMFST) columns. The specimens were manufactured by using high performance cementitious materials without using coarse aggregate. The influence of adding glass-fibres to the mix on the behavior of both axially and eccentrically loaded columns is considered. It was found that adding glass fibre improves the confinement behavior, the axial compressive strength, the stiffness and the toughness of both axially and eccentrically loaded columns. The compressive strength of axially loaded columns is compared with strength predictions according to EC4 and the AISC specification. It was found that the design predictions according to EC4 and the AISC codes provide conservative results for CMFST and GFCMFST columns. Alternatively, the axial load–bending moment interaction diagrams specified in the EC4 are conservative for the eccentrically tubular CMFST and GFCMFST tested columns.

Keywords: experimental investigation; cementitious material-filled; square hollow section; glass-fibre; axially loaded column; eccentrically loaded column

1. Introduction

Concrete-filled steel tubular (CFST) columns are considered as one of essential structural elements in both non-seismic and high seismic construction. For limited land areas, CFST columns are preferred to use whereas the use of CFST columns increases the height of buildings. The CFST column has, however, been increasingly used because of their excellent properties, namely, high stiffness, high strength, high ductility and large energy absorption capacity as discussed by Shanmugam and Lakshmi (2001), Johansson (2002) and Patel *et al.* (2016). A typical cross-section of square CFST column is illustrated in Fig. 1. Several investigations concentrated on the behavior of square and rectangular CFST members due to its easier in fabrication and installation of beam-to-column joints compared with those of circular cross-sections (Han 2004, Ellobody 2007, Wang *et al.* 2012, Jiang *et al.* 2013, Patel *et al.* 2012a, b, Liang *et al.* 2012, Chung *et al.* 2013, Qu *et al.* 2015 and Albareda-Valls and Carreras 2015). Generally, it was found that these CFST columns have much higher strengths compared with bare steel tubular columns.

Fibre reinforced concrete is still quasi-brittle in the hardened state, and yields low flow ability in the fresh state, as discussed by Srinivasa Rao and Seshadri Sekhar (2008). Recently, modifications were made to the manufacturing of the cementitious composite fibre reinforced materials by eliminating the coarse aggregate and are known as high performance fibre reinforced cementitious materials. High flowability and high percentage of strain-hardening behavior are the main characteristics of the high perform-

mance cementitious materials in the fresh and the hardening state, respectively. This progress is attributed to the developments in fibre types, used chemical admixture, matrix and in process technology. In order to understand the behavior of fibre composites many research works were devoted to studying its micromechanics; see Srinivasa Rao and Seshadri Sekhar (2008); Li *et al.* (2004) established that using glass fibres improves the mechanical properties, toughness, durability and the fire resistance. The main object for using fibres in cementitious composite is the strain-hardening after the first cracking. This leads to increasing toughness and capacity, as well as enhancing the cracking pattern and mode of failure. Although having excellent properties, high performance fibre reinforced cementitious composites have not been widely adopted in construction until now. Thus, this work presents high performance glass fibre reinforced mortar which has never been examined with present tested parameters and specimens details.

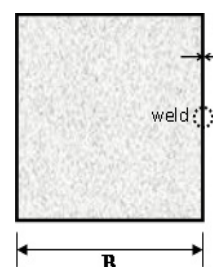


Fig. 1 Cross-section of square CFST columns

*Corresponding author, Ph.D.,
E-mail: omnia_m102010@yahoo.com

To the authors' best knowledge, the behavior of glass-fibre reinforced and unreinforced cementitious material-filled square steel tubular (GFCMFST and CMFST, respectively) columns has never been investigated, except the usage of polypropylene fibres, found in the literature of Ellobody and Ghazy (2012). Hence, in this paper, the ultimate strengths, the confinement and the behavior of GFCMFST and CMFST axially loaded columns and eccentrically loaded columns are presented. Full-scale experimental four axially loaded columns and four eccentrically loaded columns are prepared and tested to failure. The experimental results are compared with those predicted by the international design codes after its discussion.

2. Experimental programme

2.1 Test specimens and instrumentations

Four axially and four eccentrically loaded columns ((two GFCMFSTs and two CMFSTs)) were tested. The influence of adding glass-fibre on the confinement behavior and the strength of axial and eccentric cementitious material-filled tubular columns are discussed. One nominal compressive strength of 60 MPa is considered to mixes using the fibre, while a higher compressive strength of 80 MPa was used in the ordinary mix (i.e., mix without fibre). Cold-formed steel tubes with a 100 mm cross-sectional depth (B) were selected. Firstly, each tube was welded to a square end plate of 18 mm thickness. After casting the cementitious material, the top ends of the columns were cured for at least 7 days before welding another cover square plate. The details of the tested column specimens are tabulated in Table 1 and clarified in Fig. 1. Also, Table 1 provides the slenderness ratio of the columns (λ) and the eccentricity of the axial loads (e). The two ends of columns were pin-ended and each specimen was supported by two horizontal tubes to prevent the out-of-plane displacement, as can be seen in Fig. 2. On the other hand, the vertical load was applied on the top end support by an either axial or eccentric load with an eccentricity (e) from the centreline.

Table 1 Details of the tested columns

Specimen	L [mm]	L_e [mm]	B [mm]	t [mm]	λ	e [mm]	f_c [MPa]	$P_{ul,Exp}$ [kN]	$\epsilon_{lc} / \epsilon_y$
C1	1100	1185	105	1.85	39	0.0	77.5	847	1.30
C2	1100	1185	105	1.85	39	0.0	61.2*	840	1.30
C3	1400	1485	105	1.85	49	0.0	77.5	788	1.00
C4	1400	1485	105	1.85	49	0.0	61.2*	781	1.11
C5	1100	1185	99.5	1.88	41	15	77.5	771	0.32
C6	1100	1185	99.5	1.88	41	15	61.2*	755	0.30
C7	1400	1485	99.5	1.88	52	15	77.5	717	0.27
C8	1400	1485	99.5	1.88	52	15	61.2*	716	0.10

* GFCMFST

Fig. 2 presents a general view of the instrumentations with two displacement transducers (LVDT), one located at the upper plate of the column for recording the shortening and the other located at the mid-height of the column for recording the lateral deflection. In addition, four strain gauges were located at the mid-height of the column; two at each side in longitudinal and transversal directions.

2.2 Steel properties

The properties of the used cold-formed steel tube material were determined by static tension test satisfied the requirements of the Australian Standard AS 1391 (1991). The test performed using a displacement controlled universal testing machine after the coupon dimensions were prepared. Fig. 3 shows the stress-strain relationship of the steel tube material (average results of different samples were cut from the faces of the column tube). The measured values of the yield strength (f_{sy}), the ultimate strength (f_u) and the modulus of elasticity (E_s) according to a gauge length of 50 mm are 345 MPa, 380 MPa and 200 GPa, respectively. Alternatively, the increased value of the yield stress in the corner of the cold-formed steel tubes was neglected due to the counteract caused by the compressive membrane residual stresses, as mentioned by Schafer and Peköz (1998).

2.3 Cementitious material properties

The 28-day compressive strengths (f_c) for the cementitious mixtures of glass-fibre reinforced and unreinforced are 60 and 80 MPa, respectively; see Table 1. The used mixes are labeled as FC60 and C80 for reinforced glass-fibre and unreinforced cementitious material, respectively. Table 2 contains the ingredients of the used mixtures and its proportions. In order to estimate the mechanical properties, three cubes with a 100 mm width and three cylinders of 100×200 mm for each batch of the mixes were prepared. For mixes FC60 and C80, the modulus of elasticity (E_c) was found to be 33.1 GPa and 33.6 GPa, respectively.

Ordinary Portland cement CEM 1 42.5N with physical and mechanical properties satisfied the requirements of EN196-1 (2005). A pozzolanic material silica fume with silicon dioxide larger than 84% was used. Superplasticizer (Gelnium C315), meeting the requirements of ASTM C494 (type F) (2013), was used to enhance the workability of the matrixes. The used fine aggregate was siliceous river sand with a 0.5% water absorption ratio and a fineness modulus of 2.2. Synthetic glass fibres were incorporated in the cementitious matrices at 1% volume fraction with an 18 mm nominal length. The flowability was measured according

Table 2 Cementitious material mixes components in Kg/m³

Mix	f_c [MPa]	Cement	Silica fume	Sand	Water	Glenium C315	Glass- fiber content	Flow [%]
C80	77.5	1000	200	705	282	18	-	2
FC60	61.2	1000	200	705	282	22	26	22

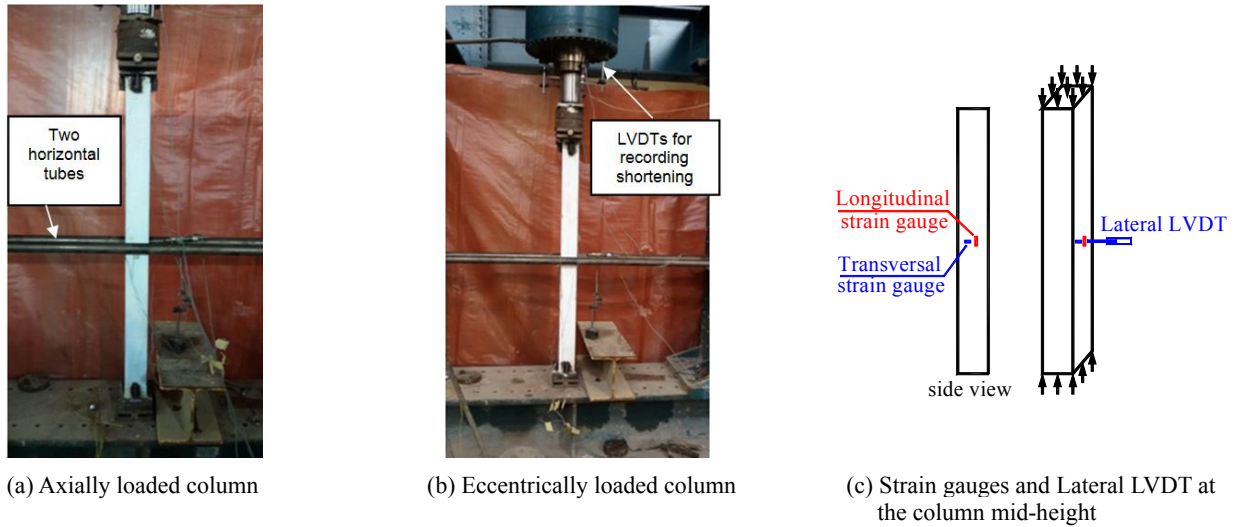


Fig. 2 Set-up and instrumentations for columns

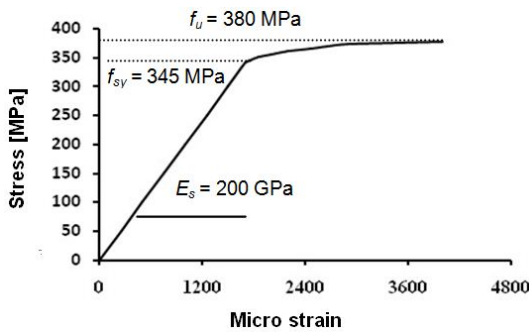


Fig. 3 Stress-strain curve of steel tube material

to ASTM C230M-14 (2014).

2.4 Columns test procedure

The set-up used for testing column specimens is seen in Fig. 2. All specimens were loaded by a hydraulic testing jack of a capacity of 2000 kN to apply compressive forces to the composite column specimens. With an increment in a load of about 25 kN, the examined column specimens were tested up to failure. The axial and eccentric loads were applied at the top loading plate by using cylindrical support to consider the pin-end supports as presented in Fig. 2. The displacement measurements and the strain readings were recorded automatically at each load increment by the data acquisition system.

3. Experimental results and discussion

3.1 General

Table 1 provides the results of the axial compressive strength of the tested specimens ($P_{ul,Exp}$). As can be seen from Table 1, the axial compressive strength for both axially and eccentrically loaded columns is nearly the same with changing the mixes from CMFSTs with C80 to GFCMFSTs with FC60. This means that adding glass fibre enhanced the compressive strength of the tested specimens



Fig. 4 Failure mode of columns

to approach the compressive strength of the high compressive strength without fibre (CMFSTs with C80). The deformed shapes of axially and eccentrically loaded columns are given in Fig. 4. It was observed that the axial column which was under compression and local buckling occurs in the faces of the axial column, indicating that the column behaves similarly to a short column. Alternatively, the deformation of the eccentric column gives the shape of a half-sine wave for pin-ended columns. In the authors' opinion, this overall buckling behavior is initiated from the early loading stage due to the eccentricity of loads.

3.2 Structural behavior

The longitudinal strain at the mid-height in the compression side of the steel tubes (ϵ_{lc}) was measured during the tests. It was compared with the strain at the yield stress of the steel material ($\epsilon_y = 0.00173$), as given in Fig. 3. The relative ratios of $\epsilon_{lc} / \epsilon_y$ are listed in Table 1. From the table, the results clarified that all current axially-loaded columns were associated with $\epsilon_{lc} / \epsilon_y$ ratios greater than unity and that the columns failed by inelastic buckling; (C1 to C4). For the case of the eccentrically-loaded columns, all the columns

failed by elastic buckling.

Figs. 5 and 6 give the relation between axial load and longitudinal strain (ϵ_l) which is measured at the middle of

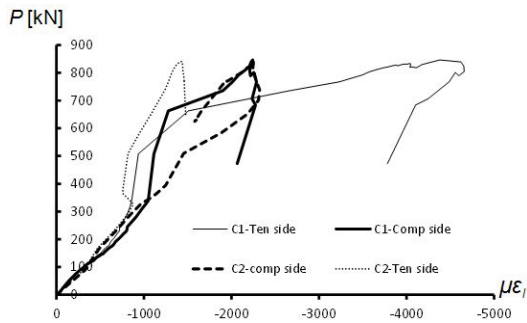


Fig. 5 Load-longitudinal strain relationships for columns C1 and C2

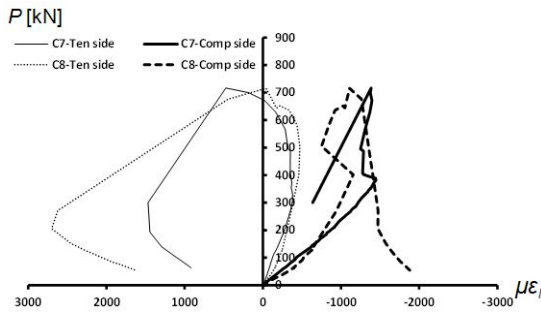
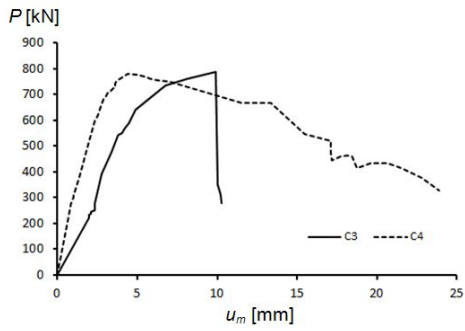


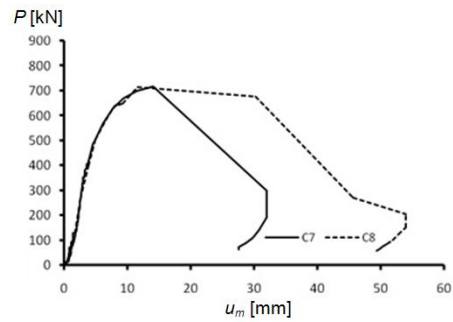
Fig. 6 Load-longitudinal strain relationships for columns C7 and C8

the mid-height sections of the steel tube in the compressive and tensile sides of the axially and eccentrically loaded columns, respectively. The negative and positive sign in strain stand for the compressive and tensile strains of the tube, respectively. For intermediate length axially loaded columns C1 and C2 as a sample of the results, it can be seen that both sides of the steel tubes were in compression. It is worth noting that the trend of this relation is the same for C3 and C4. Fig. 6 shows that, in eccentrically loaded columns C7 and C8 with a length of 1400 mm, the compression face of the steel tube was in compression and part of the tension face was located on the tension side. For the tension side at the ultimate loads, it was observed that the specimen included glass fibre (C8) is still in compression side while another unreinforced glass fibre one (C7) was in the tension side as clarified in Fig. 6. This means that adding glass fibre to the mix improved the behavior of tension and delays the cracks of the cementitious material. The descending part of the curve of specimen C8 at the tension side is gradually decreased compared with the specimen without glass fibre C7, which led to higher energy absorption of the fibre reinforced column specimens. The initial stiffness in the compression and tension sides is different from each other for the early loading stage as a result of the load eccentricity (C7 and C8).

Fig. 7 shows axial load-lateral deflection (u_m) curves of four specimens with nearly the same slenderness ratio (λ) for axially and eccentrically loaded columns. It can be observed that adding fibre to the mix-infill decreases the lateral displacement of axially loaded columns and increases

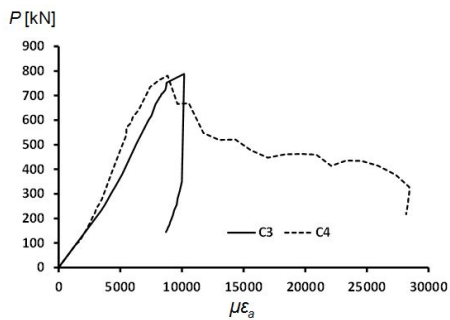


(a) Axially loaded columns

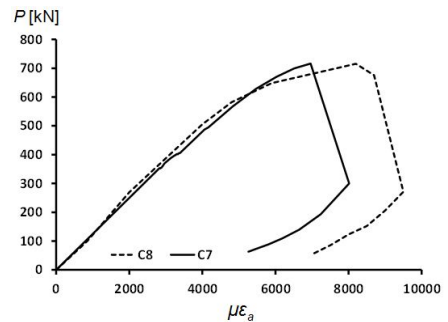


(b) Eccentrically loaded columns

Fig. 7 Load-mid-height deflection (u_m) relationships

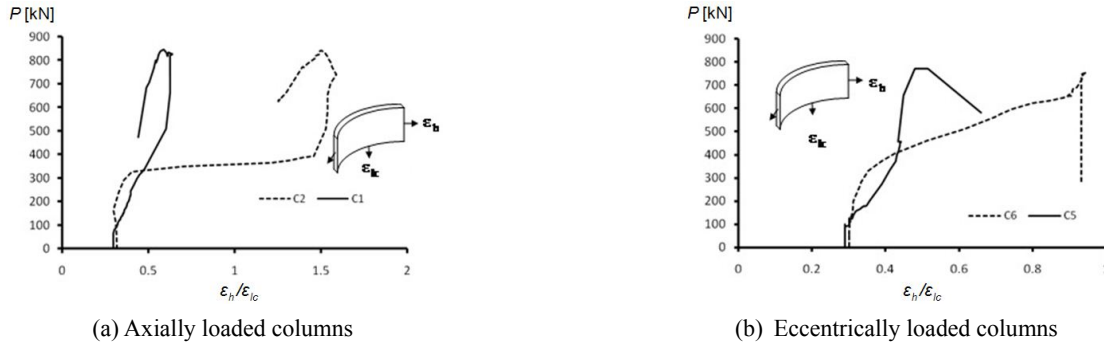


(a) Axially loaded columns



(b) Eccentrically loaded columns

Fig. 8 Load-axial strain ($\mu\epsilon_a$) relationships


 Fig. 9 Normalized load - $\varepsilon_h / \varepsilon_{lc}$ relationships for typical CFST slender columns

the initial stiffness of the column. For eccentrically loaded columns, the behavior of both CMFSTs with C80 and GFCMFSTs with FC60 is the same concerning stiffness and ultimate strength. This means that adding glass fibre to the mix enhanced the axial compression strength and initial stiffness to be nearly the same as those of the high strength concrete, as observed also in the relationships of axial load versus axial strain (ε_a); see Fig. 8.

It is worth to give an attention to the large amount of lateral deformation and strains shown in Figs. 7 and 8 for glass fibre reinforced specimens after reaching the peak load. It can be concluded that these columns have a higher toughness than the others.

The confinement of cementitious material-filled was measured from the experimental results by calculating the ratio of the hoop and longitudinal strains ($\varepsilon_h / \varepsilon_{lc}$) of the steel tube at the mid-height section of each column. Where ε_h and ε_{lc} represent the hoop and the longitudinal strains in the compression side of the steel tube, respectively. Fig. 9 shows the relationships between the axial load (P) and the ratio of $\varepsilon_h / \varepsilon_{lc}$ for axially and eccentrically loaded CMFST and GFCMFST columns. As shown in Fig. 9, the $\varepsilon_h / \varepsilon_{lc}$ ratio of the steel tube was 0.3 (Poisson effect) at the early loading stage and increased until the ultimate load was reached for the current columns. On the other hand, it can be seen that this ratio increases more in the case of GFCMFST than CMFST columns. It can be clearly seen that the confinement at the ultimate strength by the steel tube for GFCMFST columns, specimen C2, (i.e., $\varepsilon_h / \varepsilon_{lc} \approx 1.53$) was higher than that provided by the steel tube for CMFST columns, specimen C1, (i.e., $\varepsilon_h / \varepsilon_{lc} \approx 0.63$) for axially loaded columns. In addition, the confinement provided at the ultimate strength by the steel tube for GFCMFST columns, specimen C6, (i.e., $\varepsilon_h / \varepsilon_{lc} \approx 0.93$) was higher than that provided by the steel tube for CMFST columns, specimen C5, (i.e., $\varepsilon_h / \varepsilon_{lc} \approx 0.52$) for eccentrically loaded columns. It can be concluded that the confinement effect increases by adding glass fibre into the cementitious material-filled. Based on the present results the confinement was improved by about 143% and 79% due to adding glass fibre for axially and eccentrically loaded columns, respectively. On the other hand, other solutions were found in the literature for improving the confinement behaviour by using stiffened concrete-filled columns (Tao *et al.* 2005 and Dabaon *et al.* 2009). According to Dabaon *et al.* (2009), it was found that the increasing of confinement was 33% increment for

stiffened columns compared with unstiffened concrete-filled columns. Hence, it can be concluded that adding glass fibre into the cementitious material-filled is considered a good and easy solution for enhancing the confinement from time and cost perspective. More experimental investigations are needed with considering different parameters such that the variation of B/t ratio, the compressive strength of the cementitious material and the fibre volume fraction into the cementitious material-filled for the total comprehensive of confinement behavior.

4. Comparison with design strengths

4.1 Axially loaded columns

4.1.1 Eurocode 4

The slenderness of the steel tubes ($(B - 2t)/t$) exceed the maximum value of 52ε ; $\varepsilon = \sqrt{235/f_{sy}}$ according to the EC4 (2004). Therefore, the current cross-sections were classified as very slender (VS). The unfactored ultimate axial strengths of CFST specimens according to the EC4 (2004) are given by

$$P_{EC4} = \chi P_{pl,Rd} \quad (1)$$

where $P_{pl,Rd}$ is the plastic resistance to the axial compression, as follows

$$P_{pl,Rd} = A_s f_{sy} + A_c f_c \quad (2)$$

A_s is the cross-sectional area of the steel tube and A_c is the cross-sectional area of concrete, the critical buckling load is to be calculated from

$$P_{cr} = \frac{\pi^2 (EI)_e}{(KL)^2} \quad (3)$$

where KL is the effective length of the member equal to L_e from the upper and lower cylindrical supports given in Table 1 and the factor K was taken as unity for the case of pin-ended supports and $(EI)_e$ is the effective elastic flexural stiffness.

$$(EI)_e = E_s I_s + 0.6 E_c I_c \quad (4)$$

where I_s and I_c are the moment of inertial of steel tube and the concrete, respectively.

Table 3 Comparison of experimental ultimate strengths of current axial cementitious material-filled tubular columns with design strengths of codes

Column	Classification	$P_{ul,Exp}$ [kN]	P_{EC4} [kN]	$\frac{P_{ul,Exp}}{P_{EC4}}$	P_{AISC} [kN]	$\frac{P_{ul,Exp}}{P_{AISC}}$
C1	VS	847	846	1.00	851	1.00
C2	VS	840	716	1.17	729	1.15
C3	VS	788	779	1.01	805	0.98
C4	VS	781	668	1.17	694	1.13
Mean				1.09		1.07
Standard deviation				0.095		0.087

The reduction factor (χ) is to be calculated using the European strut curves as

$$\chi = 1 / (\varphi + \sqrt{\varphi^2 - \bar{\lambda}^2}) \leq 1.0 \quad (5)$$

$$\varphi = 0.5(1 + \alpha(\bar{\lambda} - 0.2) + \bar{\lambda}^2) \quad (6)$$

where $\bar{\lambda}$ is the slenderness parameter given by

$$\bar{\lambda} = \sqrt{P_{pl,Rd} / P_{cr}} \quad (7)$$

With $\alpha = 0.34$ (buckling curve (b)) for $3\% < \rho_s \leq 6\%$ which is the case of the current models; ρ_s is the ratio of the cross-sectional area of the steel tube to that of the concrete core and $\bar{\lambda}$ is the column slenderness parameter (relative slenderness).

4.1.2 AISC specification

According to the AISC specification (2010), the unfactored ultimate axial strengths (P_{AISC}) of CFST columns are given as

$$P_{AISC} = \begin{cases} \left[\begin{matrix} no \\ 0.658 \frac{P_{no}}{P_e} \end{matrix} \right] : & P \frac{P_{no}}{P_e} \leq 2.25 \\ 0.877 P_e : & \frac{P_{no}}{P_e} > 2.25 \end{cases} \quad (8)$$

$$P_{no} = \begin{cases} P_p = A_s f_{sy} + 0.85 A_c f_c & \text{For compact sections} \\ P_p - \frac{P_p - P_y}{\lambda_r - \lambda_p} (\lambda - \lambda_p)^2 & \text{For noncompact sections (9)} \\ A_s F_{cr} + 0.7 A_c f_c & \text{For slender sections} \end{cases}$$

$$P_y = A_s f_{sy} + 0.7 A_c f_c$$

$$F_{cr} = \frac{9 E_s}{(B/t)^2}$$

Where λ , λ_p , λ_r are the slenderness ratios determined from Table 11.1A of the AISC (2010) as $\lambda = B/t$,

$$\lambda_p = 2.26 \sqrt{\frac{E_s}{f_{sy}}} \text{ and } \lambda_r = 3.0 \sqrt{\frac{E_s}{f_{sy}}} \text{ and } P_e \text{ is the elastic}$$

critical buckling load determined from Eq. (3).

The above two design strengths are compared with the experimental strengths ($P_{ul,Exp}$) as illustrated in Table 3. As can be seen from the table, the strengths P_{EC4} and P_{AISC} provide conservative results for CMFST columns and more conservative results for GFCMFST columns. The main values of $P_{ul,Exp} / P_{EC4}$ and $P_{ul,Exp} / P_{AISC}$ are 1.09 and 1.07, respectively.

4.2 Eccentrically loaded columns

According to EC4 (2004), the plastic moment resistance of the composite member ($M_{PL,Rd}$) may be calculated using the assumed rectangular stress blocks as shown in Fig. 10. By using these stress blocks, $M_{PL,Rd,EC4}$ is calculated as

$$M_{PL,Rd,EC4} = M_{max,Rd} - 0.85 f_c (B - 2t) \times (h_n)^2 / 2 - f_y \left((t \times (2h_n)^2) / 4 \times 2 \right) \quad (10)$$

Where

$$M_{max,Rd} = 0.85 f_c W_{pc} / 2 + f_{sy} W_{ps} \quad (11)$$

W_{pc} is the plastic modulus of the concrete section, given by $W_{pc} = ((B - 2t) \times (D - 2t)^2) / 4$, W_{ps} is the plastic modulus of steel tube section, given by $W_{ps} = ((B \times D^2) / 4 - ((B - 2t)$

Table 4 Comparison between experimental results and EC4 (2004) for eccentrically loaded columns

Specimen	P_{EC4} [kN]	$P_{ul,Exp}$ [kN]	$\frac{P_{ul,Exp}}{P_{EC4}}$	M_{EC4} without imperfection [kN.m]	M_{EC4} with imperfection [kN.m]	$M_{ul,Exp}$ [kN.m]	$\frac{M_{ul,Exp}}{M_{EC4}}$ Consider initial imperfection
C5	764	771	1.01	4.2	8.4	11.6	1.4
C6	651	755	1.16	3.5	7.1	11.3	1.6
C7	697	717	1.03	7.2	12.1	10.8	0.9
C8	603	716	1.19	5.6	9.8	10.7	1.1
Main			1.10				1.25
Standard deviations			0.09				0.31

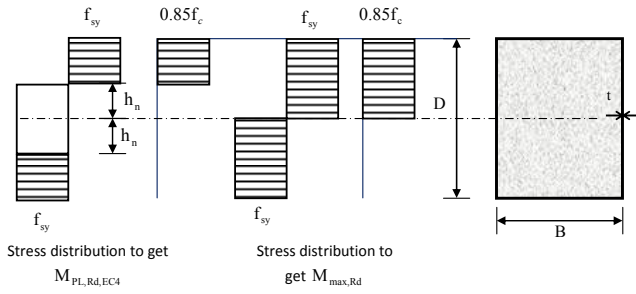


Fig. 10 Plastic stress distribution for concrete-filled cross-section under bending EC4 (2004)

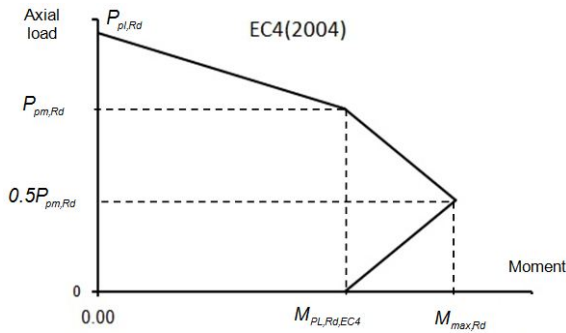


Fig. 11 EC4 interaction curve for eccentrically loaded columns

$$\times (D - 2t)^2 / 4), \text{ and } h_n = \frac{0.85f_c(B - 2t) \times (D - 2t) / 2}{0.85f_c(B - 2t) + 4t \times f_{sy}}. \text{ Note}$$

that for the current square cross-sections, the outer dimensions are equal; ($B = D$).

The load-bending moment interaction diagram according to EC4 (2004) was plotted in Fig. 11.

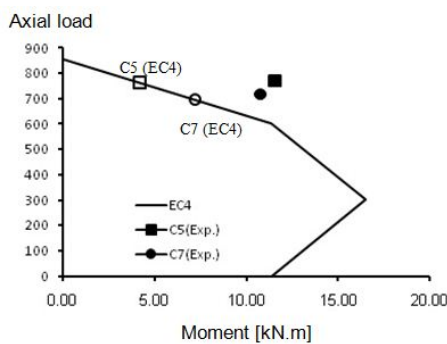
By using Eqs. (1), (10), (11) and (12) the interaction diagram could be simulated.

For the current eccentrically loaded CMFST and GFCMFST columns tested in this paper the column axial load-bending moment interaction diagrams specified in the EC4 (2004) were illustrated. Fig. 12 shows the interaction diagrams plotted for CMFST columns (C5 and C7) specimens and GFCMFST columns (C6 and C8), respectively. It can be observed that the EC4 predictions are conservative for the eccentrically tubular CMFST and

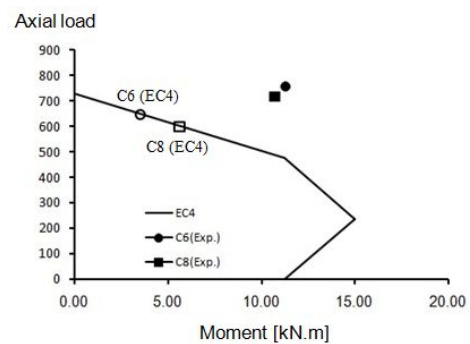
GFCMFST columns tested in this study. It is worth noting that the moment capacity of the eccentrically loaded columns depended on the axial load according to EC4 (2004) which were given in Table 4. The axial load was drawn on the axial load-bending interaction diagrams of the composite column section. Hence, the moment capacity corresponding to the axial load could be determined from the interaction diagram. It should be noted that the discrepancy between EC4 (2004) prediction and experimental results of the bending moment was due to neglecting the effect of the initial bow imperfections for composite columns which were given in Table 6.5 of EC4 (2004). On the other hand, the authors calculated the bending moment of eccentrically loaded columns again with considering the effect of the initial bow imperfections compared with the experimental results as given in Table 4. According to Table 6.5 of EC4 (2004) the member imperfection was ($L/200$) caused additional moment on the column equal to $P_{EC4} \times L/200$. The main values of $P_{ul,Exp} / P_{EC4}$ and $M_{ul,Exp} / M_{EC4}$ with considering the effects of the initial imperfection are 1.1 and 1.25 with Standard deviations of 0.09 and 0.31, respectively.

5. Conclusions

The behavior of glass-fibre reinforced and unreinforced cementitious material-filled square steel tubular (GFCMFST and CMFST, respectively) axially and eccentrically loaded columns have been investigated experimentally. Four axially and four eccentrically loaded columns (two CMFST and two GFCMFST) were tested. The strength (f_c) of the cementitious material (80 MPa) was purposely chosen much higher in the CMFST elements compared to that of the GFCMFST elements (60 MPa). It was found that adding glass fibre to the cementitious material-filled improves the confinement of cementitious material, the axial strength, the stiffness and the toughness of both centric and eccentric specimens. In addition, the axial strength of tested axially loaded columns is compared with the design strength predictions according to EC4 (2004) and the AISC (2010). The design predictions gave conservative results for CMFST axially loaded columns and more conservative for GFCMFST axially loaded columns. The moment-axial load interaction relationships according to the EC4 were calculated and compared with the experimental results of



(a) CMFST columns (C5 and C7)



(b) GFCMFST columns (C6 and C8)

Fig. 12 EC4 interaction curve for CMFST and GFCMFST columns

eccentrically loaded columns. It was found that the interaction relationships of the EC4 gave conservative results for CMFST eccentrically loaded columns and more conservative for the GFCMFST eccentrically loaded columns. Hence, in general, it can be recommended to use the design strength predictions according to EC4 for axially and eccentrically loaded CMFST and GFCMFST columns.

Acknowledgments

The authors would like to acknowledge the Faculty of Engineering, Tanta University, for its support. They are grateful to the Material Properties Laboratory and the Concrete and Heavy Structures Laboratory staff for their assistance or support during the experimental testing of the columns.

References

- AISC 360 (2010), Load and Resistance Factor Design Specification, for Structural Steel Buildings; American Institute of Steel Construction, Chicago, IL, USA.
- Albareda-Valls, A. and Carreras, J.M. (2015), "Efficiency of stiffening plates in fabricated concrete-filled tubes under monotonic compression", *Steel Compos. Struct., Int. J.*, **18**(4), 1023-1044.
- ASTM C230M-14 (2014), Standard Specification for Flow Table for Use in Tests of Hydraulic Cement.
- ASTM C494 / C494M-13 (2013), Standard Specification for Chemical Admixtures for Concrete; Annual Book of ASTM Standard.
- Australian Standard (1991), Methods for Tensile Testing of Metals; AS 1391, Standards Association of Australia, Sydney, Australia.
- Chung, K-S., Kim, J-H. and Yoo, J-H. (2013), "Experimental and analytical investigation of high-strength concrete-filled steel tube square columns subjected to flexural loading", *Steel Compos. Struct., Int. J.*, **14**(2), 133-153.
- Dabaon, M., El-Khoriby, S., El-Boghdadi, M. and Hassanein, M.F. (2009), "Confinement effect of stiffened and unstiffened concrete-filled stainless steel tubular stub columns", *J. Constr. Steel Res.*, **65**(8-9), 1846-1854.
- Ellobody, E. (2007), "Nonlinear behavior of concrete-filled stainless steel stiffened slender tube columns", *Thin-Wall. Struct.*, **45**(3), 259-273.
- Ellobody, E. and Ghazy, M.F. (2012), "Experimental investigation of eccentrically loaded fibre reinforced concrete-filled stainless steel tubular columns", *J. Constr. Steel Res.*, **76**, 167-176.
- EN 196-1:2005 (2005), Methods of Testing cement - Part 1: Determination of Strength.
- Eurocode 4 (2004), Design of Composite Steel and Concrete Structures - Part 1.1: General Rules and Rules for Buildings; British Standard Institution, London, UK, ENV 1994-1-1.
- Han, L-H. (2004), "Flexural behavior of concrete-filled steel tubes", *J. Constr. Steel Res.*, **60**(2), 313-337.
- Han, L-H., Yao, G-H. and Liao, F-Y. (2006), "Further study on the flexural behavior of concrete-filled steel tubes", *J. Constr. Steel Res.*, **62**(6), 554-565.
- Jiang, A-Y., Chen, J. and Jin, W-L. (2013), "Experimental investigation and design of thin-walled concrete-filled steel tubes subject to bending", *Thin-Wall. Struct.*, **63**, 44-50.
- Johansson, M. (2002), "Composite action and confinement effects in tubular steel-concrete columns", Ph.D. Thesis; Chalmers University of Technology, Goteborg, Sweden.
- Li, V.C., Horikoshi, T., Ogawa, A., Torigoe, S. and Saito, T. (2004), "Micromechanics-based durability study of polyvinyl alcohol-engineered cementitious composite (PVA-ECC)", *ACI Mater. J.*, **101**(1), 242-248.
- Liang, Q.Q., Patel, V.I. and Hadi, M.N.S. (2012), "Biaxially loaded high-strength concrete-filled steel tubular slender beam-columns, Part I: Multiscale simulation", *J. Constr. Steel Res.*, **75**, 64-71.
- Patel, V.I., Liang, Q.Q. and Hadi, M.N.S. (2012a), "High strength thin-walled rectangular concrete-filled steel tubular slender beam-columns, Part I: Modeling", *J. Constr. Steel Res.*, **70**, 377-384.
- Patel, V.I., Liang, Q.Q. and Hadi, M.N.S. (2012b), "High strength thin-walled rectangular concrete-filled steel tubular slender beam-columns, Part II: Behavior", *J. Constr. Steel Res.*, **70**, 368-376.
- Patel, V.I., Uy, B., Prajwal, K.A. and Aslani, F. (2016), "Confined concrete model of circular, elliptical and octagonal CFST short columns", *Steel Compos. Struct., Int. J.*, **22**(3), 497-520.
- Qu, X., Chen, Z. and Sun, G. (2015), "Axial behaviour of rectangular concrete-filled cold-formed steel tubular columns with different loading methods", *Steel Compos. Struct., Int. J.*, **18**(1), 71-90.
- Schafer, B.W. and Peköz, T. (1998), "Computational modelling of cold-formed steel: Characterizing geometric imperfections and residual stresses", *J. Constr. Steel Res.*, **47**(3), 193-210.
- Shanmugam, N.E. and Lakshmi, B. (2001), "State of the art report on steel-concrete composite columns", *J. Constr. Steel Res.*, **57**(10), 1041-1080.
- Srinivasa Rao, P. and Seshadri Sekhar, T. (2008), "Impact strength and workability behavior of glass fibre self compacting concrete", *Int. J. Mech. Solids*, **3**(1), 61-74.
- Tao, Z., Han, L.H. and Wang, Z.B. (2005), "Experimental behaviour of stiffened concrete-filled thin-walled hollow steel structural (HSS) stub columns", *J. Constr. Steel Res.*, **61**(7), 962-983.
- Wang, Y., Yang, Y. and Zhang, S. (2012), "Static behaviors of reinforcement-stiffened square concrete-filled steel tubular columns", *Thin-Wall. Struct.*, **58**, 18-31.

CC